

Lawrence Berkeley National Laboratory

LBL Publications

Title

Direct observation of spoke evolution in magnetron sputtering

Permalink

<https://escholarship.org/uc/item/1qz816d2>

Journal

Applied Physics Letters, 111(6)

ISSN

0003-6951

Authors

Anders, André

Yang, Yuchen

Publication Date

2017-08-07

DOI

10.1063/1.4994192

Peer reviewed

Accepted Manuscript.

This work was published in *Applied Physics Letters*.

Citation: *Appl. Phys. Lett.* **111**, 064103 (2017); doi: 10.1063/1.4994192

View online: <http://dx.doi.org/10.1063/1.4994192>

Free download from the above link until 10 Sept. 2017.

Direct observation of spoke evolution in magnetron sputtering

André Anders^{1,*} and Yuchen Yang,^{1,2}

¹ Lawrence Berkeley National Laboratory, 1 Cyclotron Road, Berkeley, California 94720, USA

² Institute of High Energy Physics, Chinese Academy of Sciences, 19B Yuquan Road, Shijingshan District, Beijing 100049, China

* Corresponding author, email: aanders@lbl.gov

Abstract

Ionization zones, also known as spokes, are plasma instabilities manifested as locations of intensified excitation and ionization over a sputtering magnetron's racetrack. Using a linear magnetron and a streak camera we were able to observe and quantify spoke dynamics. The technique allows us to image the onset and changes for both direct current magnetron sputtering (dcMS) and high power impulse magnetron sputtering (HiPIMS). Spokes in dcMS exhibit substructures. Spokes in HiPIMS are not stable as they shift along the racetrack, rather, they tend to grow or diminish, and they may split and merge. Their evolution can be interpreted in the context of localized electric fields and associated electron heating.

Acknowledgments

We thank Joe Wallig for with help setting up the system, and Shuo Xu and Sebastien Tetaud for assistance in some of the imaging setups. The Kurt J. Lesker Company kindly provided the linear magnetron. This work was done at Lawrence Berkeley National Laboratory with support by the U.S. Department of Energy, under Contract No. DE-AC02-05CH11231.

Sputtering magnetrons are widely used to produce thin films and coatings. While the technology is generally considered mature, recent research in magnetrons' plasma properties showed the richness of plasma instabilities. Magnetrons generally, but not always, exhibit ionization zones,^{1,2} also known as “spokes” in analogy to well-known $\mathbf{E} \times \mathbf{B}$ instabilities of Hall thrusters.³ Spokes are generally needed to help facilitate electron current flow from the closed $\mathbf{E} \times \mathbf{B}$ drift path to the anode⁴ (\mathbf{E} and \mathbf{B} are the local electric and magnetic field vectors). Spokes can be found in high power impulse magnetron sputtering (HiPIMS),^{1,2} as well as in the more traditional direct current magnetron sputtering (dcMS).⁵ In HiPIMS, spokes drift in the $\mathbf{E} \times \mathbf{B}$ direction, i.e. the direction of the electron drift. In contrast, spokes drift in the opposite direction for dcMS, indicating that at least two opposing mechanisms are responsible for the motion or shift of spokes. Briefly, one can argue that a spoke shift in the $-\mathbf{E} \times \mathbf{B}$ direction (as observed in dcMS) should be the expected, the “natural” direction, because drifting electrons arriving at a spoke are accelerated at the spoke edge's electric field,⁶ while ions formed there are accelerated in the $-\mathbf{E} \times \mathbf{B}$ direction, displacing the electric double layer in the $-\mathbf{E} \times \mathbf{B}$ direction. Additionally, those ions are subsequently accelerated to the target where they emit secondary electrons on the $-\mathbf{E} \times \mathbf{B}$ side of the spoke's edge.⁶ In dcMS there are always plenty (gas) neutrals available to be ionized by energetic electrons, however, the situation is different in HiPIMS: neutrals may be locally depleted due to rarefaction and intense ionization. As was argued in ref.¹, neutrals can locally be depleted by ionization in spokes, and ions will be depleted (“evacuated”) by the local electric field. As a result, electrons arriving at a HiPIMS-spoke have to drift a bit further in the $\mathbf{E} \times \mathbf{B}$ direction to encounter neutrals to be ionized. That implies a displacement of the most intense ionization in the $\mathbf{E} \times \mathbf{B}$ direction. At intermediate current levels, between dcMS and HiPIMS, spoke direction reversal can be observed.^{7,8}

Additional information on spokes has been gained by numerous probe studies, including those monitoring the potential distribution of dcMS spokes,⁶ the merging and splitting of spokes in HiPIMS,⁹ and simultaneous oscillations of the potential of all spokes, labeled as “breathing mode”.¹⁰

In this contribution we add a powerful approach to such research by using a “linear” magnetron, i.e. a magnetron with straight sections of the racetrack, and projecting one of the straight sections

onto the entrance slit of a streak camera. While optical measurements and imaging has been done before, here we can directly follow the evolution of spokes as they move along the racetrack.

The experiments make use of a linear planar magnetron (Kurt J. Lesker Comp.) with a 240 mm × 120 mm target. The target thickness can be selected using a suitable clamping frame: Al, Ti, and Cu targets of 3.1 mm and 6.2 mm thickness (1/8" and 1/4") were used, however, in this paper we focus on the results with a 3.1 mm thick aluminum target only; the other results will be presented in a more comprehensive report. The magnetic field was mapped in detail but here it should suffice to state that the strongest magnetic field component in the target plane, 1 mm over a 3.1 mm thick target, was 80 mT.

The setup is shown in Fig. 1: the magnetron was mounted inside in a stainless-steel high vacuum chamber of 1 m inner diameter, cryogenically pumped to a base pressure in the low 10^{-5} Pa range. Argon, and in some cases argon mixed with oxygen or nitrogen, was introduced at a flow rate of 100 sccm with different gate valve positions to the cryogenic pump adjusting the pumping speed in order to obtain a desired pressure, typically 0.4 Pa. The magnetron was placed in the center of the chamber facing a 20 cm diameter (8") glass window for taking images with a fast-shutter or a fast streak camera. The chamber window had a shutter which was kept closed unless an image was taken. For space reasons, we focus on the streak camera results in the Letter, and will elaborate on more results in an upcoming paper.

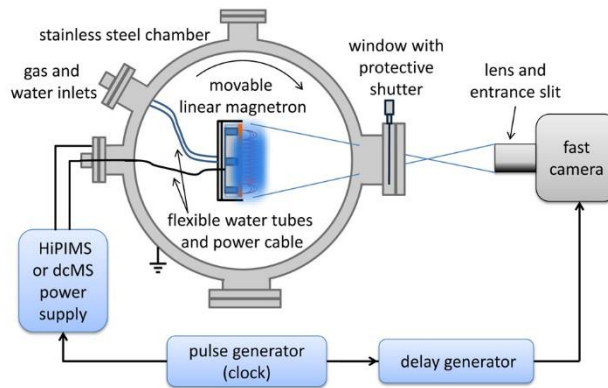


FIG. 1. Experimental setup: One of the straight sections of the linear magnetron was projected by the lens onto the entrance slit of the streak camera, allowing us to observe the evolution of spokes as they move along that section of the magnetron's racetrack.

The discharge was powered by a high current pulse generator, model SIPP2000USB (Melec GmbH), capable of delivering pulses up to 1 kV and up to 1000 A of arbitrary duration from 5 μ s up to 1000 μ s (or even longer for low peak power). This power supply can also serve as a dc power supply (i.e., without pulsing). In its “unipolar negative” mode, the pulser delivers negative pulses to the target, with the anode connected to ground. Typical pulse lengths were 20-1000 μ s with repetition rates between 200 and 10 Hz. The supply’s arc threshold was usually set to 990 A to allow for high current pulses without the arc detection to kick in. We always recorded the target voltage and made sure that the magnetron operated in the magnetron mode, not in the arc mode. Arcs, if present, can be easily recognized by their much lower cathode-anode voltage than the voltage of magnetron discharges. To monitor the voltage, a 100:1 voltage divider probe (model P5100 by Tektronix) was attached to the power feedthrough. The discharge current was recorded using a current transformer (model 101 by Pearson) when operating with pulsed discharges, and using a dc volt meter (Fluke 189) across a low-impedance shunt resistor when investigating dcMS. All electrical signals were recorded with a fast 4-channel digital oscilloscope (Tektronix TDS5104B).

Two camera types were employed, a gated Intensified Charged Coupled Device (ICCD) camera (model PIMAX 4 by Princeton Instruments), and a streak camera (model C7700 by Hamamatsu), equipped with an $f = 135$ mm Nikon lens and detector module C4742-98 whose spectral response is in the range 300-1060 nm. The images of the PIMAX camera served to show that spokes on a linear magnetron look like the spokes on a round magnetron. With that established, we can focus on the streak camera results because the slit geometry can be matched to one of the two straight sections of the racetrack.

A streak camera is distinct from a conventional camera as light enters the camera through a slit and is recorded in time. Compared to conventional cameras, one sacrifices resolution in one space direction but gains resolution in time. Streak images are space-time (x,t) presentation of light intensity, as opposed to space-space (x,y) images obtained by conventional cameras.

The part of the target projected onto the streak camera entrance slit was 1 mm wide and 20 cm long. A comprehensive set of streak and fast-shutter camera images has been acquired for magnetron plasmas operating at various currents, pressures, target materials and target thicknesses: we will show and discuss here a few selected streak images only, namely those that are either characteristic and/or provide particular insight. All images show the intensity of light emitted from

the plasma presented in the false color scale “royal” of the image processing software IMAGEJ.¹¹ As it is intuitively clear, black is the least intense and white the most.

We start with images in dcMS. As we know from probe measurements and fast frame camera imaging,^{5,8,12} certain power and pressure conditions lead to one, two, or more spokes that are relatively stable as they move along the racetrack, while other parameter combinations exhibit less stability. Fig. 2 shows a spoke moving from left to right, in the $-\mathbf{E}\times\mathbf{B}$ direction: the most interesting observation here is that the spoke has substructures that move in the opposite direction. From the slope one can immediately determine the velocities: on average about 1500 m/s for the main spoke, and at least 10,000 m/s for the substructures. The exact values vary somewhat. The main spoke seems to accelerate about 20 μs into the image, and then stalls for 10 μs before resuming its travel to the right. About 80 μs into this image, the main spoke moves out of the observation window and 10 μs later the next spoke appears from the left.

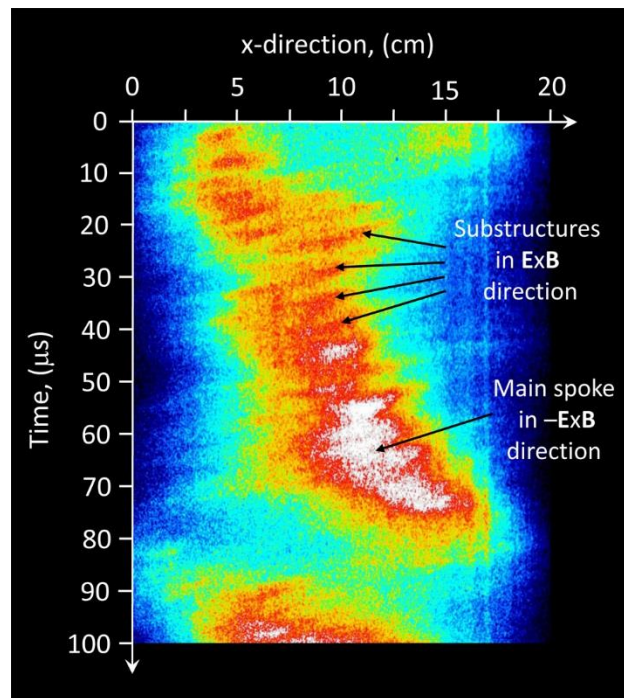


FIG. 2. Spoke of a dcMS discharge, 1 A at 280 V, Al target, in 0.4 Pa argon. The spoke moves from left to right (in $-\mathbf{E}\times\mathbf{B}$) while substructures have a different tilt, hence move in the opposite direction. (Here, and in all other images: vertical lines, especially on the right, are due to defects in the camera’s phosphorous and thus artifacts: they should be disregarded.)

Going to higher currents will increase ionization and we may reach the region where the before-mentioned competing spoke drift mechanisms cancel or where one or the other dominates, as evident by direction changes of spoke drift. Fig. 3 shows such situation when using a higher current compared to Fig. 2.

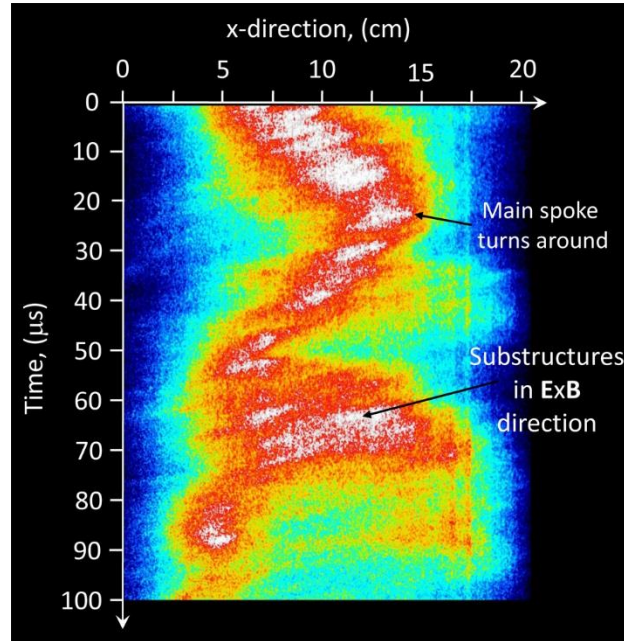


FIG. 3. Spoke of a dcMS discharge, 3 A at 313 V, Al target, in 0.4 Pa argon. The main spoke changes direction; substructures moving in the $\mathbf{E} \times \mathbf{B}$ direction are also evident.

Figures 2 and 3 show the example of an aluminum target in argon. Images taken with titanium and copper targets are qualitatively similar to images with an aluminum target, which is not too surprising since the plasma and the emitted light in dcMS is dominated by gas species.

The situation is quite different in HiPIMS. Here, the images depend very much on the target material as it determines the composition of the plasma, at least at later times in each HiPIMS pulse.^{4,13} At the very beginning of each pulse, for several microseconds after the visible onset of plasma generation, the plasma appears uniform but quickly, within microseconds, develops spokes. Figure 4 illustrates that for the case of aluminum in nitrogen for a pulse that eventually will reach 900 A after 200 μs .

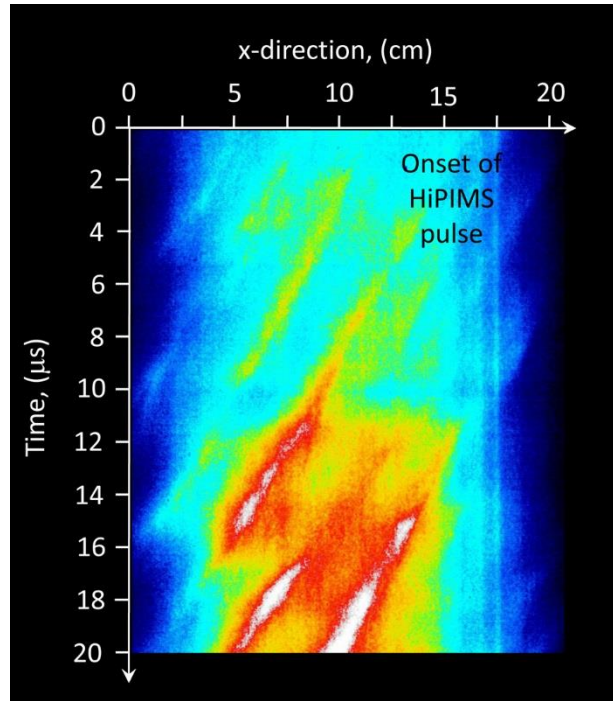


FIG. 4. Spokes of a HiPIMS discharge, applied voltage 547 V (later in the pulse leading to 900 A peak), Al target, in 0.4 Pa Ar with 16 mPa N₂ added, image taken at the beginning of the pulse. Spokes already develop after several microseconds; they move in the $\mathbf{E} \times \mathbf{B}$ direction (from right to left). Note that the image amplifier setting is much reduced compared to the settings of figures 2 and 3.

Later in the pulse we find evidence for (i) pattern-formation (self-organization) expressed by approximate equal distance between spokes, and (ii) significant variability or dynamics of spokes (Fig. 5). Figure 5 was taken under the same pulse condition as conditions of Fig. 4 but about in the middle of the 200 μs pulse. One can see that spokes gain and lose intensity. While the trailing edges move with relatively constant and equal velocity, energetic electrons leaving the spoke (see the * symbol in the figure) “catch up” with the preceding spoke and amplifying it.

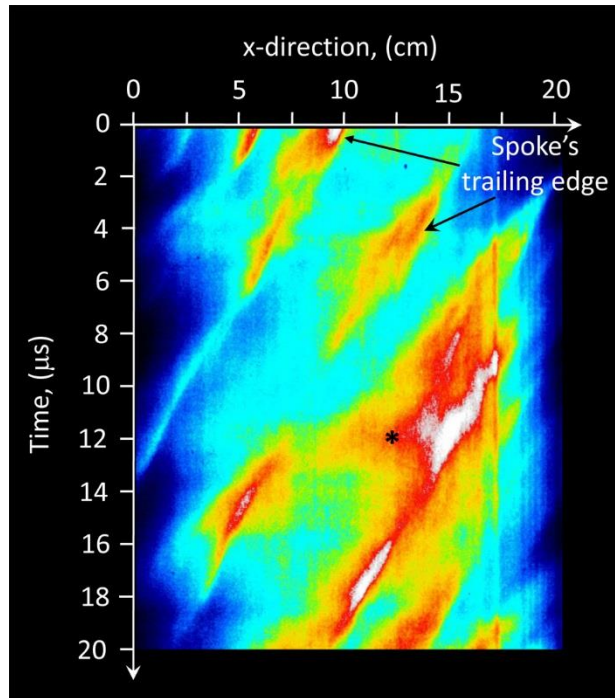


FIG. 5. Spoke of a HiPIMS discharge, applied voltage 547 V (later in the pulse leading to 900 A peak), Al target, in 0.4 Pa Ar with 16 mPa N₂ added, image taken near the middle of the pulse. The * symbol indicates where energetic electrons leave the spoke and “catch up” with the preceding spoke (to the left), amplifying it.

Spoke dynamics remains evident throughout the entire pulse. Figure 6 shows a 20 μs window near the end of the 200 μs HiPIMS pulse, also taken under the same discharge conditions as in Figs. 4 and 5. This figure contains also an example for spoke splitting.

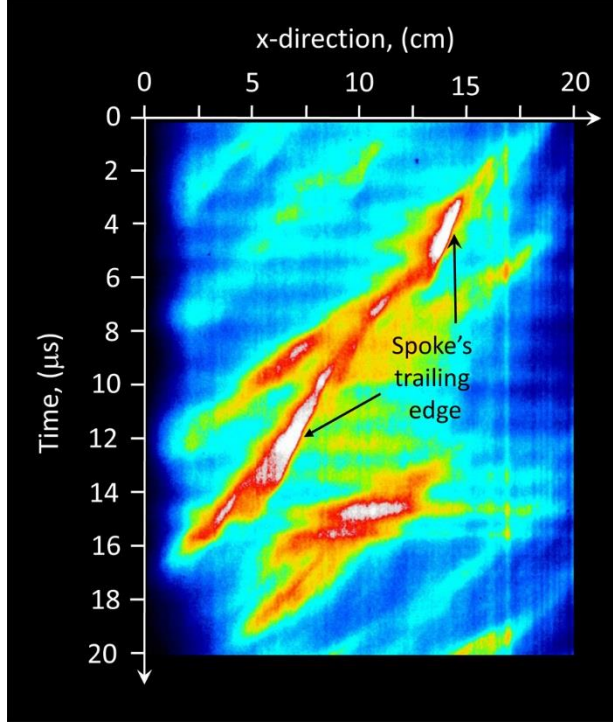


FIG. 6. Spoke of a HIPIMS discharge, applied voltage 547 V (leading to 900 A peak at the end of the pulse), Al target, in 0.4 Pa Ar with 16 mPa N₂ added. We see an example of spoke splitting at about 8 μs into the image. The horizontal brightness modulations correlate with oscillations of discharge current, which often occur near the end of each pulse.

To interpret these images we should recall that we record light which is directly correlated with the density of excited states of atoms and ions. In the following we consider gas atoms for simplicity, and the expressions for other species are analogous. Electrons populating the upper level of optical transitions are usually pumped into these upper levels by electron impact excitation. The excitation frequency is proportional to the density of atoms, n_A , in the ground state and to the capability of electrons to pump electrons to the upper level:

$$\nu_{0u} = n_A \int \sigma_{0u}(v_e) v_e f(v_e) dv_e \quad (1)$$

where σ_{0u} is the velocity dependent cross section, v_e is the electron velocity, and $f(v_e)$ is the electron velocity distribution function (equivalently, one could write (1) as an energy-dependent expression). In the case of dcMS, especially at low current, n_A is approximately constant everywhere (apart from some rarefaction near the target). The gas density greatly exceeds the density of electrons, and the light intensity is therefore not determined by the presence of neutrals

but by the electrons' ability to cause excitation and ionization. More intense light emission is thus an indication for a greater density of electrons energetic enough to pump ground state electrons into excited states. The presence of distinct regions of greater excitation and ionization, the spokes, are therefore a visual indicator for the distribution of the electron energy, or more to the point, the localization of electron heating, as proposed in earlier papers interpreting gated camera images.^{14,15}

The excitation location can be slightly different than the location of radiative de-excitation due to the finite lifetime of excited states, characterized by Einstein coefficients of spontaneous emission. These times are usually shorter than 1 μ s and therefore the displacement of atoms while they are excited can be estimated to be 1 mm or less. In other words, in the context of this discussion, the location of excitation is approximately the location of spontaneous emission.

Considering the images related to dcMS, figures 2 and 3, we see substructures that can be related to groups of energetic electrons drifting in the $\mathbf{E} \times \mathbf{B}$ direction with a velocity of slightly more than 1×10^4 m/s. Assuming that the electron drift is dominated by the $\mathbf{E} \times \mathbf{B}$ drift mechanism, and further considering that the B-field some mm above the target is about 50 mT, the electric field in the magnetic presheath is, on average, of the order 500 V/m, a reasonable value.⁶ Energetic electrons cause ionization and excitation (the shape and position of the corresponding cross sections are similar), and electrons drift away from the locations of ionization faster than ions are removed by the local electric field, thus the plasma potential is locally enhanced where more ionization occurs. This, in turn, is the mechanism that gives electrons arriving at his location the extra "kick" in energy, allowing them to cause inelastic collisions.

There is no obvious reason why the potential structure of spokes in dcMS and HiPIMS are fundamentally different. Also here, now considering HiPIMS, the locations of enhanced light emission presumably are the locations where electrons are more energetic, i.e. where electrons are "heated" by moving into locations of higher potential. The difference to dcMS is the rate of ionization, excitation, and degree of ionization, which can lead to strong depletion of neutrals by rarefaction and ionization. Considering equation (1), the density n_A is now a function of location. The events leading to excitation and ionization depend on both the presence of particles to be excited and ionized and the energy of electrons of these locations. That makes the system much more complicated and cause the greater dynamics of spokes in HiPIMS. Indeed, stable spoke

configurations, with exactly one or two or more spokes can be found in dcMS⁶ while in HiPIMS, spokes may occasionally form a self-organized patterns^{1,16,17} but generally show greater variability, including spoke splitting and merging.⁹

In summary, spoke evolution has been studied using a linear magnetron and a streak camera, which opens the special opportunity to follow spoke evolution. In contrast to previous studies with round target magnetrons, the spoke remains in view while travelling in a straight section, allowing us to observe substructures in dcMS spokes, and merging and splitting of spokes in HiPIMS. The observations can be interpreted considering the energetics of electrons responsible for excitation and ionization. The local character of spokes indicates a local character of electron energization, which can be associated with the local structure of the plasma potential. Regions of greater light emissions are locations of greater electron energy, which consistently should be regions of higher potential. Such interpretation is supported by earlier reports on spectral imaging¹⁴ and emissive probe measurements.⁶

Figure Captions

FIG. 1. Experimental setup: One of the straight sections of the linear magnetron was projected by the lens onto the entrance slit of the streak camera, allowing us to observe the evolution of spokes as they move along that section of the magnetron's racetrack.

FIG. 2. Spoke of a dcMS discharge, 1 A at 280 V, Al target, in 0.4 Pa argon. The spoke moves from left to right (in $-\mathbf{E} \times \mathbf{B}$) while substructures have a different tilt, hence move in the opposite direction. (Here, and in all other images: vertical lines, especially on the right, are due to defects in the camera's phosphorous and thus artifacts: they should be disregarded.)

FIG. 3. Spoke of a dcMS discharge, 3 A at 313 V, Al target, in 0.4 Pa argon. The main spoke changes direction; substructures moving in the $\mathbf{E} \times \mathbf{B}$ direction are also evident.

FIG. 4. Spokes of a HIPIMS discharge, applied voltage 547 V (later in the pulse leading to 900 A peak), Al target, in 0.4 Pa Ar with 16 mPa N₂ added, image taken at the beginning of the pulse. Spokes already develop after several microseconds; they move in the $\mathbf{E} \times \mathbf{B}$ direction (from right to left). Note that the image amplifier setting is much reduced compared to the settings of figures 2 and 3.

FIG. 5. Spoke of a HIPIMS discharge, applied voltage 547 V (later in the pulse leading to 900 A peak), Al target, in 0.4 Pa Ar with 16 mPa N₂ added, image taken near the middle of the pulse. The * symbol indicates where energetic electrons leave the spoke and "catch up" with the preceding spoke (to the left), amplifying it.

FIG. 6. Spoke of a HIPIMS discharge, applied voltage 547 V (leading to 900 A peak at the end of the pulse), Al target, 0.4 Pa Ar with 16 mPa N₂ added. We see an example of spoke splitting at about 8 μ s into the image. The horizontal brightness modulations correlate with oscillations of discharge current, which often occur near the end of each pulse.

References

- ¹ A. Anders, P. Ni, and A. Rauch, "Drifting localization of ionization runaway: Unraveling the nature of anomalous transport in high power impulse magnetron sputtering," *J. Appl. Phys.* **111**, 053304 (2012).
- ² A. P. Ehiasarian, A. Hecimovic, T. de los Arcos, R. New, V. Schulz-von der Gathen, M. Böke, and J. Winter, "High power impulse magnetron sputtering discharges: instabilities and plasma self-organization," *Appl. Phys. Lett.* **100**, 114101 (2012).
- ³ J. P. Boeuf, "Tutorial: Physics and modeling of Hall thrusters," *J. Appl. Phys.* **121**, 011101 (2017).
- ⁴ A. Anders, "Tutorial: Reactive High Power Impulse Magnetron Sputtering (R-HiPIMS)," *J. Appl. Phys.* **121**, 171101 (2017).
- ⁵ A. Anders, P. Ni, and J. Andersson, "Drifting ionization zone in sputtering magnetron discharges at very low currents," *IEEE Trans. Plasma Sci.* **42**, 2578 (2014).
- ⁶ M. Panjan and A. Anders, "Plasma potential of a moving ionization zone in DC magnetron sputtering," *J. Appl. Phys.* **121**, 063302 (2017).
- ⁷ Y. Yang, J. Liu, L. Liu, and A. Anders, "Propagation direction reversal of ionization zones in the transition between high and low current magnetron sputtering," *Appl. Phys. Lett.* **105**, 254101 (2014).
- ⁸ A. Hecimovic, C. Maszl, V. Schulz-von der Gathen, M. Böke, and A. von Keudell, "Spoke rotation reversal in magnetron discharges of aluminium, chromium and titanium," *Plasma Sources Sci. Technol.* **25**, 035001 (2016).
- ⁹ P. Klein, F. L. Estrin, J. Hnilica, P. Vašina, and J. W. Bradley, "Simultaneous electrical and optical study of spoke rotation, merging and splitting in HiPIMS plasma," *J. Phys. D: Appl. Phys.* **50**, 015209 (2017).
- ¹⁰ Y. Yang, X. Zhou, J. X. Liu, and A. Anders, "Evidence for breathing modes in direct current, pulsed, and high power impulse magnetron sputtering plasmas," *Appl. Phys. Lett.* **108**, 034101 (2016).
- ¹¹ W. Rasband, *ImageJ 1.44p*, downloaded from <http://imagej.nih.gov/ij> (National Institute of Health, 2011).
- ¹² M. Panjan, S. Loquai, J. E. Klemberg-Sapieha, and L. Martinu, "Non-uniform plasma distribution in dc magnetron sputtering: origin, shape and structuring of spokes," *Plasma Sources Sci. Technol.* **24**, 065010 (2015).
- ¹³ M. Hála, O. Zabeida, B. Baloukas, J. E. Klemberg-Sapieha, and L. Martinu, "Time- and species-resolved plasma imaging as a new diagnostic approach for HiPIMS discharge characterization," *IEEE Trans. Plasma Sci.* **38**, 3035 (2010).
- ¹⁴ J. Andersson, P. Ni, and A. Anders, "Spectroscopic imaging of self-organization in high power impulse magnetron sputtering plasmas," *Appl. Phys. Lett.* **103**, 054104 (2013).
- ¹⁵ A. Anders, "Localized heating of electrons in ionization zones: Going beyond the Penning-Thornton paradigm in magnetron sputtering," *Appl. Phys. Lett.* **105**, 244104 (2014).

- ¹⁶ A. Hecimovic, N. Britun, S. Konstantinidis, and R. Snyders, "Sputtering process in the presence of plasma self-organization," *Appl. Phys. Lett.* **110**, 014103 (2017).
- ¹⁷ A. Anders, "Self-organization and self-limitation in high power impulse magnetron sputtering," *Appl. Phys. Lett.* **100**, 224104 (2012).